Physics Letters B 668 (2008) 277–281

Contents lists available at ScienceDirect

Physics Letters B

www.elsevier.com/locate/physletb

Effects of orbital occupancies on the neutrinoless $\beta\beta$ matrix element of ^{76}Ge

J. Suhonen [a,*], O. Civitarese [b]

[a] Department of Physics, University of Jyväskylä, PO Box 35, FIN-40014, Jyväskylä, Finland
[b] Department of Physics, University of La Plata, c.c. 67, (1900) La Plata, Argentina

ARTICLE INFO

Article history:
Received 20 February 2008
Received in revised form 13 August 2008
Accepted 19 August 2008
Available online 2 September 2008
Editor: W. Haxton

PACS:
21.60.Jz
23.40.Bw
23.40.Hc
27.50.+e

Keywords:
Neutrinoless double beta decay
Nuclear matrix elements
Orbital occupancies

ABSTRACT

In this work we use the recently measured neutron occupancies in the ^{76}Ge and ^{76}Se nuclei as a guideline to define the neutron quasiparticle states in the 1p0f0g shell. We define the proton quasiparticles by inspecting the odd-mass nuclei adjacent to ^{76}Ge and ^{76}Se. We insert the resulting quasiparticles in a proton–neutron quasiparticle random-phase approximation (pnQRPA) calculation of the nuclear matrix element of the neutrinoless double beta ($0\nu\beta\beta$) decay of ^{76}Ge. A realistic model space and effective microscopic two-nucleon interactions are used. We include the nucleon–nucleon short-range correlations and other relevant corrections at the nucleon level. It is found that the resulting $0\nu\beta\beta$ matrix element is smaller than in the previous pnQRPA calculations, and closer to the recently reported shell-model results.
© 2008 Published by Elsevier B.V.

The neutrinoless double beta ($0\nu\beta\beta$) decay of atomic nuclei plays a key role in the search for massive Majorana neutrinos and their mass scale [1–6]. To extract the necessary information from the measured data [7–9] the nuclear-structure effects have to be accounted for by computation of the associated nuclear matrix elements (NME's). Here we discuss the NME's for the light-neutrino exchange mechanism.

One most often uses the proton–neutron quasiparticle random-phase approximation (pnQRPA) [3,4,10] to treat the structure of double-beta decaying nuclei. Also recent shell-model results are available [11–14]. The pnQRPA is a model tailored to describe the energy levels of odd–odd nuclei and their beta decays to the neighboring even–even nuclei [15]. Also its extension, renormalized pnQRPA [16], has been used [17,18] to compute double-beta matrix elements. The pnQRPA (and the renormalized pnQRPA) contains a free parameter, the so-called particle–particle strength parameter, $g_{\rm pp}$, that controls the magnitude of the proton–neutron two-body interactions in the $T=0$ pairing channel [19,20]. The fixing of the value of this parameter has been done either by using the data on two-neutrino double beta ($2\nu\beta\beta$) decay [18] or the data on single beta decay [21,22].

The pnQRPA calculations are based on quasiparticle states [15] produced via a BCS calculation [23]. The BCS method gives occupations of the single-particle orbitals and the occupation amplitudes are connected to the energy differences between orbitals. The customary way to determine the single-particle energy difference is to use the Woods–Saxon mean-field potential [23]. Slight adjustments of the resulting energies can be done based on the data on energy levels of odd-mass nuclei in the neighbourhood of the nucleus where the pnQRPA calculation is done [24].

Recently the single-particle occupancies in the ^{76}Ge and ^{76}Se nuclei were measured by (p,t) reactions [25]. As a result, the vacancies in the neutron subspace 1p-0f$_{5/2}$-0g$_{9/2}$, hereafter called the pfg subspace, could be deduced. In this work we exploit this spectroscopic data in pnQRPA calculations of the nuclear wave functions of the ^{76}As nucleus, the intermediate nucleus in the double beta decay of ^{76}Ge. We first produce the $2\nu\beta\beta$ NME to fix the allowed values of the $g_{\rm pp}$ parameter by data on the half-life of the decay.[1] Based on this we finally compute the $0\nu\beta\beta$ NME's.

Here we assume that the double beta decay of ^{76}Ge proceeds through the virtual states of the intermediate nucleus ^{76}As to the ground state of the final nucleus ^{76}Se. By assuming the neutrino-

* Corresponding author.
E-mail address: jouni.suhonen@phys.jyu.fi (J. Suhonen).

[1] Since ^{76}Ge lacks single beta decay data we use the $2\nu\beta\beta$ data to fix the possible values of $g_{\rm pp}$.

0370-2693/$ – see front matter © 2008 Published by Elsevier B.V.
doi:10.1016/j.physletb.2008.08.056

Table 1
WS single-particle energies for the pfg subspace in units of MeV

Orbital	^{76}Ge		^{76}Se	
	Neutrons	Protons	Neutrons	Protons
$1p_{3/2}$	−11.52	−9.015	−12.77	−7.000
$0f_{5/2}$	−10.72	−8.212	−11.98	−6.288
$1p_{1/2}$	−9.797	−6.789	−10.98	−5.001
$0g_{9/2}$	−7.030	−5.311	−8.305	−3.371

mass mechanism to be the dominant one, we can write the inverse of the half-life for the $0\nu\beta\beta$ decay as [3]

$$\left[t_{1/2}^{(0\nu)}\right]^{-1} = G_1^{(0\nu)}\left(\frac{\langle m_\nu\rangle}{m_e}\right)^2 \left(M^{(0\nu)}\right)^2, \tag{1}$$

where m_e is the electron mass and $G_1^{(0\nu)}$ is the leptonic phase-space factor. The $0\nu\beta\beta$ nuclear matrix element $M^{(0\nu)}$ consists of the Gamow–Teller, Fermi and tensor parts as

$$M^{(0\nu)} = M_{GT}^{(0\nu)} - \left(\frac{g_V}{g_A}\right)^2 M_F^{(0\nu)} + M_T^{(0\nu)}. \tag{2}$$

Our numerical calculations verify the shell-model results of [14] and show that the tensor part in (2) is quite small and its contribution can be safely neglected in what follows. The expressions for the phase-space factor, the effective neutrino mass $\langle m_\nu\rangle$ and the matrix elements of (2) are given, e.g., in [1,3,10].

The nuclear-structure calculations are performed as described in [26–28]. As a model space we have used the $N = 3$ and $N = 4$ oscillator shells and the $0h_{11/2}$ single-particle orbital, both for protons and neutrons. The starting values of the single-particle energies are obtained from the Coulomb-corrected Woods–Saxon potential, hereafter called WS, with the parametrization of [29]. These energies are presented for the pfg subspace in Table 1. The measured neutron vacancies [25] in this sub-space have been summarized in Table 2. As can be seen from this table, the computed vacancies in the WS basis are far from the measured ones: the $0g_{9/2}$ orbital is much too thinly occupied and the other orbitals are too full.

The pnQRPA calculation of the wave functions of ^{76}As needs as input the neutron and proton occupation amplitudes in the pfg subspace. Instead of using the WS based BCS amplitudes for neutrons we now resort to the occupation amplitudes derived from the measured vacancies of Table 2. It is then interesting to see to what extent this choice of occupation amplitudes affects the magnitudes of the computed double beta decay NME's.

We have to stress here that in this work we compute the occupancies of the neutron orbitals at the BCS level. Though effects beyond pairing may be present in the observed occupancies, in the present calculation we identify them with pair correlations, treated by the use of BCS. This can be justified partly by the good agreement between the calculated and observed properties of the low-lying energy levels in the adjacent odd-mass nuclei. Further support can be sought from calculations that determine the orbital occupancies and the pnQRPA amplitudes X and Y self-consistently [30]. In [30] this kind of scheme was applied in a realistic model space to study Fermi pn excitations in ^{76}Ge. From Fig. 5 of [30] one can see that the occupancies of the neutron orbitals in the pfg subspace do not change significantly when the BCS + pnQRPA results are replaced by the self-consistent results. The proton Fermi surface sharpens a bit when going from the BCS + pnQRPA over to the self-consistent approach of [30], but the effect is quite small (anyway, we do not have experimental occupancies available for protons).

No data on proton spectroscopic factors in the pfg subspace exist for ^{76}Ge or ^{76}Se. The computed proton vacancies in the WS basis are given in Table 3. One possible way to access the needed

Table 2
Measured and WS based neutron vacancies in the pfg subspace

Orbital	^{76}Ge		^{76}Se	
	Exp.	WS	Exp.	WS
$\nu 1p_{1/2} + \nu 1p_{3/2}$	1.13	0.357	1.59	0.495
$\nu 0f_{5/2}$	1.44	0.500	2.17	0.618
$\nu 0g_{9/2}$	3.52	5.43	4.20	7.06

Table 3
Predicted proton vacancies in the pfg subspace. The calculations were done in the WS and adjusted basis

Orbital	^{76}Ge		^{76}Se	
	Adj.	WS	Adj.	WS
$1p_{1/2}$	1.82	1.80	1.70	1.62
$1p_{3/2}$	2.19	1.92	1.75	1.44
$0f_{5/2}$	4.58	4.43	3.80	3.32
$0g_{9/2}$	9.28	9.73	8.61	9.49

occupations for protons is to compute the spectra of the proton-odd nuclei ^{77}As and ^{77}Br, adjacent to ^{76}Ge and ^{76}Se. For this one can use the quasiparticle–phonon coupling in diagonalizing the residual nuclear Hamiltonian. If one takes the phonons to be pnQRPA phonons one ends up with a scheme called the proton–neutron microscopic quasiparticle–phonon model (pnMQPM) [31]. The pnMQPM wave function consists of a linear combination of one-quasiparticle and three-quasiparticle components. A one-quasiparticle state in this scheme is a state whose wave function is dominated by a definite one-quasiparticle component.

Comparing the energies of the computed one-quasiparticle states with the available data gives information on the quality of the underlying BCS calculation and thus on the mean-field single-particle energies. The pnMQPM computed proton one-quasiparticle states in ^{77}As and ^{77}Br are given in Table 4. The wave functions corresponding to these states are indeed dominated by a single one-quasiparticle component. This is visible from the contribution of this component to the total normalization of the wave function, as presented by the percentage in the last column of the table.

The predicted one-quasiparticle energies of Table 4 correspond nicely to their measured counterparts. The critical proton orbit for the success of the pnMQPM calculation is $\pi 0g_{9/2}$. The energy of this orbit had to be lowered to −7.1 MeV for ^{76}Ge and to −5.3 MeV for ^{76}Se to produce a reasonable one-quasiparticle spectrum. The corresponding energies we call adjusted energies and the computed proton vacancies in this basis are given in Table 3 in the columns called 'Adj.'. Comparison of Tables 2 and 3 indicates that the adjusted proton and experimental neutron vacancies behave qualitatively in the same way. However, the adjustments on the proton side have not such drastic effects on the vacancies as is the case on the neutron side when going from the WS to the experimental vacancies. For completeness, we also give in Table 4 the computed and measured energies of the neutron one-quasiparticle states in ^{77}Ge and ^{77}Se. Here the basis, adjusted independently of the pnMQPM calculation, shifts the $9/2^+$ state slightly below the measured $1/2^-$ state. Related to this one has to bear in mind that such very fine details of odd-mass spectra are hard to reproduce within a quasiparticle–phonon coupling scheme.

The main point of the present Letter is to see how the neutron vacancies of the pfg subspace, extracted from experimental data, affect the magnitude of the $0\nu\beta\beta$ NME's. As a side line one can also try to relate the measured vacancies to the single-particle energies of this subspace. The WS potential is a global parametrization of the nuclear mean field and is based on data on nuclei close to the beta stability line. This potential produces a smooth and gentle variation of the single-particle energies as a function of the proton and neutron numbers. On the other hand,

Table 4
One-quasiparticle states in odd-A nuclei near ^{76}Ge and ^{76}Se. In the last column the contribution to the total normalization is given in per cents

Nucleus	State	E(exp.) [MeV]	E(th.) [MeV]	Main component (%)
^{77}Ge	$1/2^-$	0.160	0.193	$\nu 1p_{1/2}$ (94.7%)
	$9/2^+$	0.225	0.000	$\nu 0g_{9/2}$ (97.0%)
^{77}As	$3/2^-$	0–0.215	0.014	$\pi 1p_{3/2}$ (95.6%)
	$5/2^-$	0.246	0.000	$\pi 0f_{5/2}$ (92.5%)
	$9/2^+$	0.475	0.471	$\pi 0g_{9/2}$ (86.5%)
^{77}Se	$1/2^-$	0.000	0.227	$\nu 1p_{1/2}$ (93.6%)
	$9/2^+$	0.175	0.000	$\nu 0g_{9/2}$ (97.6%)
	$3/2^-$	0.239	0.677	$\nu 1p_{3/2}$ (85.5%)
	$5/2^-$	0.250	0.506	$\nu 0f_{5/2}$ (93.0%)
^{77}Br	$3/2^-$	0.000	0.083	$\pi 1p_{3/2}$ (98.5%)
	$9/2^+$	0.106	0.072	$\pi 0g_{9/2}$ (93.3%)
	$5/2^-$	0.162	0.000	$\pi 0f_{5/2}$ (95.3%)
	$1/2^-$	0.167	0.426	$\pi 1p_{1/2}$ (87.6%)

Table 5
Matrix elements of (3) computed in this work for different values of g_A and g_{pp}. For the short-range correlations both the Jastrow and UCOM prescriptions have been used

		Jastrow			UCOM		
g_A	g_{pp}	$(M^{(0\nu)}_{GT})'$	$(M^{(0\nu)}_{F})'$	$(M^{(0\nu)})'$	$(M^{(0\nu)}_{GT})'$	$(M^{(0\nu)}_{F})'$	$(M^{(0\nu)})'$
1.25	1.12	2.288	−0.772	2.779	3.385	−1.143	4.112
1.00	1.10	1.700	−0.579	2.279	2.413	−0.818	3.231

Table 6
Values of the matrix element $(M^{(0\nu)})'$ of (3) obtained in some other recent works. Here (J) stands for Jastrow and (U) for UCOM

g_A	(J) [28]	(U) [28]	(J) [35,36]	(U) [36]	(J) [14]	(U) [14]
1.25	4.029	5.355	4.68	5.73	2.30	2.81
1.00	3.249	4.195	3.33	3.92	–	–

the WS potential is just an approximate substitute for the Hartree–Fock (HF) or Hartree–Fock–Bogoliubov (HFB) methods to calculate the self-consistent mean field. The HF and HFB methods can produce results that are very different from those of the WS potential. Their results are also very much dependent on the two-body interaction used in the calculations (for recent articles on these features see [32,33]).

In [32] a discussion of the $N = 40$ and $Z = 40$ mean-field gaps between the $1p_{1/2}$ and $0g_{9/2}$ single-particle orbitals was carried out by using the HF method with two different two-body interactions. Let us first discuss the situation for protons. It was found that on the proton side for one of the interactions, VMS (see Fig. 15 of [32]), the gap between the $1p_{1/2}$ and $0g_{9/2}$ orbitals disappeares around $Z = 34$ and the two orbitals become inverted in energy. For the other interaction, JW (see Fig. 16 of [32]), the gap between these two orbitals diminishes when going from $Z = 26$ to $Z = 48$ but never disappears. Thus the VMS-computed mean field closely corresponds to our adjusted proton basis where the gap between the $1p_{1/2}$ and $0g_{9/2}$ orbitals disappears.

On the neutron side the VMS based HF calculation from $N = 24$ to $N = 48$ produces a clear gap between the $1p_{1/2}$ and $0g_{9/2}$ orbitals, as seen in Fig. 3 of [32]. However, in [32] it was found that the effect of this gap disappeared when the $T = 1$, $J = 0$ pairing interaction was added through the HFB method. If one would like to simulate these vacancies in the present simple WS + BCS calculations the WS mean field should be modified such that the gap at $N = 40$ closes.

At this point it has to be stressed, however, that in the present work we do not have to resort to the details of the underlying mean field and the associated neutron single-particle energies since we have already the experimental vacancies available. Some further insight in the complexity of the self-consistent mean-field calculations for Ge isotopes is given in [33]. There several standard interactions were used in the Gogny–HFB and Skyrme–HF + BCS frameworks and very different results, from triaxial to axially symmetric shapes, were obtained with different interactions for ^{76}Ge. In fact, looking at the simple Nilsson diagram indicates that a tiny oblate deformation would suffice to close the $N = 40$ gap.

After settling the problem with the occupation amplitudes of the single-particle states we are ready to compute the $2\nu\beta\beta$ and $0\nu\beta\beta$ NME's. As usual, we consider the two extreme values of the axial-vector coupling constant, namely the bare value $g_A^b = 1.25$ and the strongly quenched value $g_A = 1.00$. When calculating the $0\nu\beta\beta$ half-lives it is convenient to remove the g_A dependence from the phase-space factor by redefining the NME as

$$\mathrm{NME}' = \mathrm{NME}\left(\frac{g_A}{g_A^b}\right)^2. \tag{3}$$

These redefined nuclear matrix elements are the ones that are listed in Tables 5 and 6.

In Table 5 we list the adopted g_{pp} values as extracted by comparing the measured $2\nu\beta\beta$ half-lives with the computed ones. By using these values of g_{pp} we have calculated the $0\nu\beta\beta$ NME's of (3) and we summarize their values in Table 5. In these calculations we have included the higher-order terms of nucleonic weak currents and the nucleon's finite-size corrections in the way described in [18,34]. We have accounted for the short-range correlations by the Jastrow and UCOM (unitary correlation operator method) correlators, as discussed, e.g. in [26–28].

Our computed results of Table 5 can be compared with the results of other recent works in the field. A selection of recent calculations including the Jastrow and the UCOM correlator is given in Table 6. The second and third columns of this table give the results of [28] where exactly the same methods as here were applied, the only difference being the use of a different set of single-particle energies, where the neutron $0g_{9/2}$ orbital was shifted a good one MeV to better reproduce the low-energy spectra of ^{77}Ge and ^{77}Se in a BCS calculation. By comparing the results of these two calculations in Tables 5 and 6 one notices a significant reduction in the value of the total $0\nu\beta\beta$ matrix element $M^{(0\nu)}$. Furthermore, the Tübingen results [35,36] are consistent with the results of [28].

The results of the shell model [14] are the smallest in Table 6. Interestingly, our present results for the Jastrow correlator, $(M^{(0\nu)})' = 2.779$, and for the UCOM correlator, $(M^{(0\nu)})' = 4.112$, are closer to the shell-model result than the previous values quoted in [28]. The reduction of the magnitude of the pnQRPA calculated NME, which yields a value close to the shell-model result, is significant and deserves the further detailed study performed below.

The reason for the reduction of the magnitude of the $0\nu\beta\beta$ NME can be summarized by looking at the multipole decomposition of the NME. As an example we use the Jastrow correlated NME's. For the Fermi matrix element the reduction stems from the 0^+ intermediate states, as seen in Fig. 1. From Fig. 2 we see that for the Gamow–Teller matrix element $M^{(0\nu)}_{GT}$ the significant changes concentrate on the 1^+ and 2^- contributions. In the present calculations the 1^+ and 2^- contributions are $0.448(1^+)$ and $0.388(2^-)$ whereas in the previous work [28] they read $0.712(1^+)$ and $0.899(2^-)$. Thus the 1^+ contribution has reduced by 37% and the 2^- contribution by 56%. In the old calculation the contribution of the 2^- was dominant but now it has reduced below the 1^+ contribution. In both calculations the 1^+ multipole has several important contributions whereas the 2^- contribution is coming almost solely from the first 2^- state. Hence the wave function of the 2^-_1 state plays a key role when seeking the reason

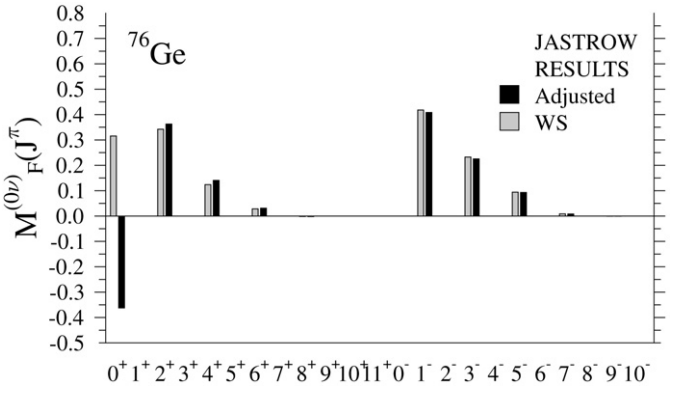

Fig. 1. Multipole decomposition of the Fermi matrix element with Jastrow short-range correlations. The black bars correspond to the modified neutron and proton occupations.

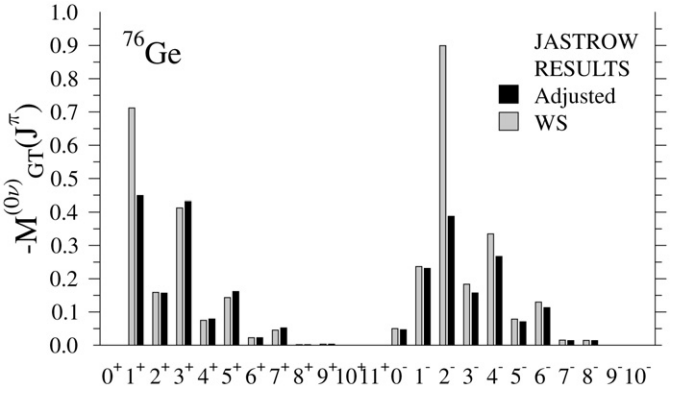

Fig. 2. The same as Fig. 1 for the Gamow–Teller matrix element.

Table 7
Beta-minus decay $\log ft$ values for transitions from the $2^-_{g.s.}$ of ^{76}As to the ground state and one- and two-phonon states in ^{76}Se

	$0^+_{g.s.}$	2^+_1	0^+_2	2^+_2	4^+_1
Exp.	9.7	8.1	10.3	8.2	11.1
Present calc.	9.7	7.4	9.0	8.4	10.7
[28]	9.0	7.7	9.2	8.7	10.9

for the reduction of the magnitude of the Gamow–Teller matrix element.

The quality of the lowest 2^- state in the intermediate nucleus ^{76}As can be tested by computing the β^- decay $\log ft$ values for transitions from this state to the ground state and one- and two-phonon states in ^{76}Se. The obtained results are compared with the data and the calculations of [28] in Table 7. As can be seen there is a drastic improvement in the $\log ft$ value of the ground-state-to-ground-state transition. This transition tests exclusively the 2^-_1 wave function whereas the rest of the transitions depend also on the final-state wave function, built from the 2^+_1 collective phonon in the ^{76}Se nucleus. It is worth pointing out that in the present calculation the quasiparticle spectrum is more compressed than in the calculation of Ref. [28]. This increases the collectivity of the 2^+_1 state in ^{76}Se and thus results in smaller effective charges when trying to reproduce the data on the E2 transition probability from this state.

The single β^- decay is a non-trivial way to check the reduction in the $0\nu\beta\beta$ NME: The β^- NME is reduced by 58% from the old value [28]. This is in nice agreement with the 56% reduction in the 2^- contribution to the $0\nu\beta\beta$ NME. The main component of the wave function driving both transitions is the proton $0f_{5/2}$ orbital coupled to the neutron $0g_{9/2}$ orbital. In the present calculation the wave function of the 2^-_1 state is more fragmented and thus reduces the pnQRPA amplitude responsible for the transitions. On the other hand, the occupation of the neutron $0g_{9/2}$ orbital has increased which also reduces the decay amplitudes since they are proportional to the emptiness of $\nu 0g_{9/2}$. Similar considerations, though in a more complicated way, apply to the intermediate 1^+ contribution.

Our calculations show that the main contributions to the $0\nu\beta\beta$ NME come from inside the pfg subspace. The implementation of the experimental occupations in the pnQRPA calculation brings the pnQRPA results closer to the shell-model results of [14]. The small contributions from outside the pfg subspace partly explain the deviations from the shell model result. In [37] the effect of expanding the shell-model single-particle basis was examined. Using the pfg subspace plus two-particle–two-hole excitations from the $0f_{7/2}$ orbital it was concluded that these 2p–2h excitations increase the magnitude of $M^{(0\nu)}$ by at most 20%. It still remains an open question how the differences between the shell-model and pnQRPA matrix elements tie to the omitted single-particle orbitals in the shell model and the shell-model occupations of the pfg subspace.

Finally, our presently computed variations $(M^{(0\nu)})' = 2.279$–2.779 (Jastrow) and $(M^{(0\nu)})' = 3.231$–4.112 (UCOM) in the $0\nu\beta\beta$ NME can be converted to the following half-life limits

$$t^{(0\nu)}_{1/2} = (5.36\text{–}8.04) \times 10^{24}\ \text{yr}/\big(\langle m_\nu\rangle[\text{eV}]\big)^2 \quad \text{(Jastrow)}, \tag{4}$$

$$t^{(0\nu)}_{1/2} = (2.45\text{–}4.00) \times 10^{24}\ \text{yr}/\big(\langle m_\nu\rangle[\text{eV}]\big)^2 \quad \text{(UCOM)}. \tag{5}$$

In this Letter we have performed a pnQRPA calculation of the nuclear matrix elements involved in the neutrinoless double beta decay of ^{76}Ge. We have used a microscopic two-nucleon interaction in a realistic model space, and the calculations exploit the occupation amplitudes extracted from the recently available data on the neutron vacancies in ^{76}Ge and ^{76}Se. The subsequently calculated $0\nu\beta\beta$ nuclear matrix elements are smaller in magnitude than the ones obtained in a standard calculation using the Woods–Saxon based single-particle occupations. This stems from the reduction in the contributions of the 0^+, 1^+ and 2^- intermediate states, with a special emphasis on the first 2^- state. These changes are related both to the revised occupations and to the changes in the pnQRPA amplitudes that derive from the revised occupations.

Acknowledgements

This work has been partially supported by the National Research Council (CONICET) of Argentina and by the Academy of Finland under the Finnish Centre of Excellence Programme 2006-2011 (Nuclear and Accelerator Based Programme at JYFL). We thank also the EU ILIAS project under the contract RII3-CT-2004-506222. One of the authors (O.C.) gratefully thanks for the warm hospitality extended to him at the Department of Physics of the University of Jyväskylä, Finland. We acknowledge the very fruitful discussions with Prof. J.P. Schiffer. We also thank Dr. M. Kortelainen and Mr. M.T. Mustonen for making their computer codes available to us.

References

[1] M. Doi, T. Kotani, E. Takasugi, Prog. Theor. Phys. Suppl. 83 (1985) 1.
[2] J.D. Vergados, Phys. Rep. 133 (1986) 1.
[3] J. Suhonen, O. Civitarese, Phys. Rep. 300 (1998) 123.
[4] A. Faessler, F. Šimkovic, J. Phys. G 24 (1998) 2139.
[5] H.V. Klapdor-Kleingrothaus, in: Springer Tracts in Modern Physics, vol. 163, Springer, Berlin, 2000, pp. 69–104.
[6] J.D. Vergados, Phys. Rep. 361 (2002) 1.
[7] V. Tretyak, Y. Zdesenko, At. Data Nucl. Data Tables 80 (2002) 83.
[8] S.R. Elliott, J. Engel, J. Phys. G 30 (2004) R183.
[9] F.T. Avignone III, S.R. Elliott, J. Engel, Rev. Mod. Phys. 80 (2008) 481, arXiv: 0708.1033.

[10] T. Tomoda, Rep. Prog. Phys. 54 (1991) 53.
[11] E. Caurier, et al., Rev. Mod. Phys. 77 (2005) 427.
[12] E. Caurier, F. Nowacki, A. Poves, Int. J. Mod. Phys. E 16 (2007) 552.
[13] E. Caurier, J. Menéndez, F. Nowacki, A. Poves, Phys. Rev. Lett. 100 (2008) 052503.
[14] J. Menéndez, A. Poves, E. Caurier, F. Nowacki, arXiv: 0801.3760 [nucl-th].
[15] J. Suhonen, From Nucleons to Nucleus: Concepts of Microscopic Nuclear Theory, Springer, Berlin, 2007.
[16] J. Toivanen, J. Suhonen, Phys. Rev. Lett. 75 (1995) 410.
[17] J. Toivanen, J. Suhonen, Phys. Rev. C 55 (1997) 2314.
[18] V.A. Rodin, A. Faessler, F. Šimkovic, P. Vogel, Nucl. Phys. A 766 (2006) 107.
[19] P. Vogel, M.R. Zirnbauer, Phys. Rev. Lett. 57 (1986) 3148.
[20] O. Civitarese, A. Faessler, T. Tomoda, Phys. Lett. B 194 (1987) 11.
[21] J. Suhonen, Phys. Lett. B 607 (2005) 87.
[22] O. Civitarese, J. Suhonen, Phys. Lett. B 626 (2005) 80;
O. Civitarese, J. Suhonen, Nucl. Phys. A 761 (2005) 313.
[23] J. Suhonen, T. Taigel, A. Faessler, Nucl. Phys. A 486 (1988) 91.
[24] M. Aunola, J. Suhonen, Nucl. Phys. A 602 (1996) 133.
[25] S.J. Freeman, et al., Phys. Rev. C 75 (2007) 051301(R);
J.P. Schiffer, private communication.
[26] M. Kortelainen, O. Civitarese, J. Suhonen, J. Toivanen, Phys. Lett. B 647 (2007) 128.
[27] M. Kortelainen, J. Suhonen, Phys. Rev. C 76 (2007) 024315.
[28] M. Kortelainen, J. Suhonen, Phys. Rev. C 75 (2007) 051303(R);
J. Suhonen, M. Kortelainen, Int. J. Mod. Phys. E 17 (2008) 1.
[29] A. Bohr, B.R. Mottelson, Nuclear Structure, vol. I, Benjamin, New York, 1969.
[30] A. Mariano, J.G. Hirsch, Phys. Rev. C 61 (2000) 054301.
[31] M.T. Mustonen, J. Suhonen, Phys. Lett. B 657 (2007) 38.
[32] K. Kaneko, M. Hasegawa, T. Mizusaki, Y. Sun, Phys. Rev. C 74 (2006) 024321.
[33] Lu Guo, J.A. Maruhn, P.-G. Reinhard, nucl-th/0701095.
[34] F. Šimkovic, G. Pantis, J.D. Vergados, A. Faessler, Phys. Rev. C 60 (1999) 055502.
[35] V.A. Rodin, A. Faessler, F. Šimkovic, P. Vogel, Nucl. Phys. A 793 (2007) 213 (Erratum).
[36] F. Šimkovic, A. Faessler, V. Rodin, P. Vogel, J. Engel, arXiv: 0710.2055 [nucl-th].
[37] E. Caurier, F. Nowacki, A. Poves, Eur. Phys. J. A 36 (2008) 195.